

This is the peer reviewed version of the following article: D. Roca-López, U. Uria, E. Reyes, L. Carrillo, K. A. Jørgensen, J. L. Vicario, P. Merino, **Mechanistic Insights into the Mode of Action of Bifunctional Pyrrolidine-Squaramide-Derived Organocatalysts**, Chem. Eur. J. 2016, 22, 884-889, which has been published in final form at <https://doi.org/10.1002/chem.201504705>.

This article may be used for non-commercial purposes in accordance with Wiley Terms and Conditions for Self-Archiving.

# Mechanistic Insights in the Mode of Action of Bifunctional Pyrrolidine-Squaramide-derived Organocatalysts

David Roca-López,<sup>[a]</sup> Uxue Uria,<sup>[b]</sup> Efraim Reyes,<sup>[b]</sup> Luisa Carrillo,<sup>[b]</sup> Karl Anker Jørgensen,<sup>[c]</sup> Jose L. Vicario<sup>\*[b]</sup> and Pedro Merino<sup>\*[a]</sup>

**Abstract:** The modes of catalytic action of three squaramide-derived bifunctional organocatalysts have been investigated using DFT methods. The [5+2] cycloaddition between oxidopyrillium ylides and enals has been used as model reaction. Two primary modes are possible for the different catalysts studied. The preference for one mode over the other is due to the possibility of additional favourable  $\pi,\pi$ -interactions between the H-bond activated pyrillium ylide and an electron-deficient aromatic ring bonded to a squaramide NH-group. The model can be extended to other reactions catalyzed by the same catalysts such as formal [2+2] cycloadditions between nitroalkenes and  $\alpha,\beta$ -unsaturated aldehydes. The computational results are in excellent concurrence with the available experimental reports on the observed total enantioselectivity and differences in diastereoselectivity depending on the substrate and the reaction.

Enantioselective C-C bond formation by means of catalytic processes is an important goal in organic synthesis<sup>[1]</sup> and understanding of the catalytic mechanism can help process optimization.<sup>[2]</sup> The use of metal-free organocatalysts enables the efficient and high enantioselective synthesis of valuable chiral intermediates. Over the last 15 years, organocatalytic reactions have been extensively studied.<sup>[3]</sup> In particular, bifunctional organocatalysts have played a prominent role in the development of enantioselective organocatalysis.<sup>[4]</sup> As enzymes, bifunctional organocatalysts bind reactants (and also transition states) via covalent and non-covalent interactions. The simultaneous activation of two species, at a low entropic cost, contributes to create a synergistic effect leading to highly stereoselective reactions.

The combination of an amino function and a group capable of forming H-bonds in one single catalyst is the most common arrangement employed in bifunctional organic catalysis. In this context a large variety of thioureas incorporating amino functionalities have been reported, making such a class of

molecules the paradigm of bifunctional organocatalysis.<sup>[5]</sup> Recently, squaramides have been proposed as an alternative to thioureas in organocatalysis<sup>[6]</sup> and consequently some examples of bifunctional organocatalysis bearing a squaramide unit have been described.<sup>[7]</sup> In 2012, two squaramide-derived bifunctional catalysts **1** and **2** were reported, specifically designed for addressing remote reactivity through H-bond directed dienamine catalysis (Figure 1).<sup>[8]</sup> Catalyst **1** provided excellent yields and enantioselectivities in dienamine-mediated inverse-demand hetero Diels-Alder reactions,<sup>[9]</sup> Michael-Henry tandem reactions<sup>[10]</sup> and Diels-Alder cycloadditions with anthracenes.<sup>[11]</sup> On the other hand, catalyst **2** showed a great efficiency in enantioselective [5+2] cycloaddition between oxidopyrillium ylides and enals, under the same type of bifunctional dienamine/H-bonding activation.<sup>[12]</sup> Finally, both **1** and **2** have been successfully used in [2+2] cycloadditions between  $\alpha,\beta$ -unsaturated aldehydes and nitroolefins,<sup>[8]</sup> and in trienamine-mediated [4+2] cycloadditions,<sup>[13]</sup> compound **1** being usually preferred for developing the reaction.

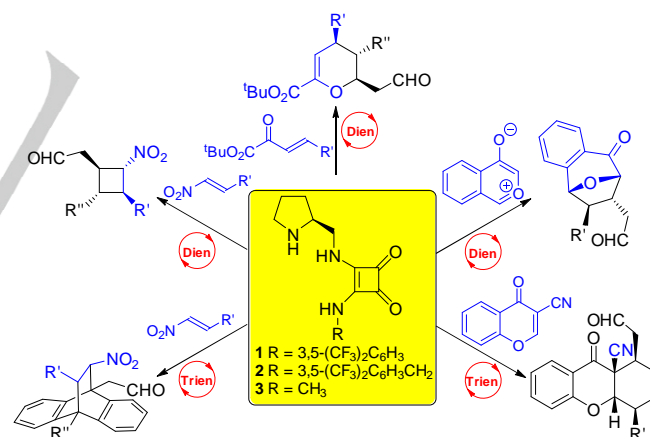


**Figure 1.** The reactivity of bifunctional pyrrolidine/squaramide catalysts **1** and **2** in organocatalytic reactions with enals and dienals (omitted for clarity) and simplified catalyst **3** used as model for preliminary calculations.

The mechanism of Diels-Alder reactions organocatalyzed by **1** has been computationally studied.<sup>[14]</sup> In this work, it was demonstrated that the high enantioselectivity exerted by **1** comes from the high distortion energy required for the catalyst to keep the dual H-bond interaction in the non-preferred pathway. Several models have been proposed in which the typical interactions have been considered, i.e. formation of the dienamine and activation through H-bonding of the squaramide.<sup>[8,13b]</sup> However, these models have not considered the role of the aromatic moiety at the terminal squaramide nitrogen. The presence of a bis(trifluoromethyl)phenyl group, as

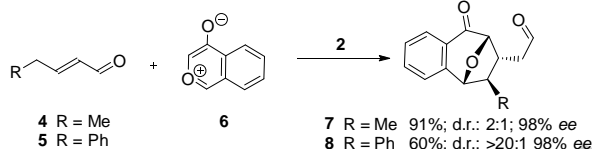
[a] D. Roca-López and Prof. Dr. P. Merino  
Laboratorio de Síntesis Asimétrica. Instituto de Síntesis Química y Catálisis Homogénea (ISQCH)  
Universidad de Zaragoza-CSIC  
Campus San Francisco, 5009 Zaragoza (Spain)  
E-mail: pmerino@unizar.es

[b] Dr. U. Uria, Dr. E. Reyes, Dr. L. Carrillo, Prof. Dr. J. L. Vicario  
Department of Organic Chemistry II  
University of the Basque Country (UPV/EHU)  
P.O. Box 644, 48080 Bilbao (Spain)  
E-mail: joseluis.vicario@ehu.es

[c] Prof. Dr. K. A. Jørgensen  
Department of Chemistry  
Aarhus University  
8000 Aarhus C (Denmark)

in catalyst **1**, could contribute to form additional non-covalent interactions such as  $\pi,\pi$ -interactions with unsaturated systems. Moreover, in the case of catalyst **2** the additional methylene group could provide additional flexibility to facilitate a correct orientation leading to additional cooperative interactions.

Herein, we report a detailed computational study directed to investigate the origin of the diastereo- and enantioselectivity provided by catalysts **1** and **2** with a special focus on the role of the arylmethyl group of **2**. For that purpose we selected the [5+2] cycloaddition between oxidopyrylium ylides and enals catalyzed by **2** as model system (Scheme 1). These studies will show that catalyst **2** adopts a disposition similar to an enzymatic pocket that put together the reagents favouring the reactivity between them, in a similar way to an enzyme does. Our computational studies employed the real catalysts **1** and **2** as well as aldehydes **4** and **5**. Optimizations of the geometries of stationary points were carried out at B3LYP-D3BJ/Def2SVP level of theory, followed by single point calculations at the B3LYP-D3BJ/Def2TZVP level.<sup>[15]</sup> Solvent effects were examined by the PCM implicit solvation model. The calculations predict complete enantioselectivity for the reaction catalyzed by **2** in all cases. Also, they predict correctly the moderate and complete diastereoselectivities observed for R = Me and Ph, respectively.

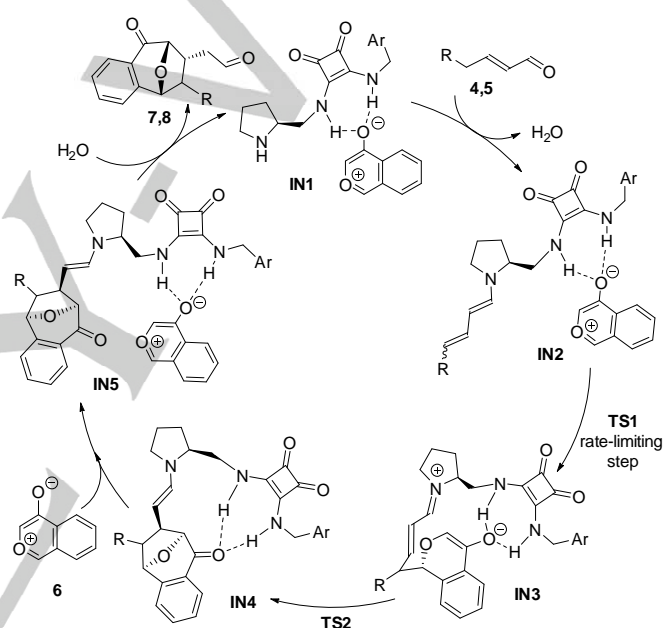


**Scheme 1.** The catalytic and enantioselective [5+2] cycloaddition<sup>[12]</sup> catalyzed by **2** employed as case study in this work.

We first studied model systems formed from pyrrolidine and (*E*)-2-pentenal **4** to determine the concertedness of the reaction. This simplest model showed the reaction to be concerted. However, when the squaramide moiety was introduced by considering compound **3** (see Figure 1) as a simple model of the chiral organocatalyst, the reaction resulted to be a stepwise process consisting of an initial attack of the dienamine to the position 1 of the ylide followed by an intramolecular Michael addition in the intermediate iminium-ion derivative. In this two-steps process the first attack of the dienamine was identified as the rate limiting step. The ultimate reason for the observed mechanism switch is the stabilization of zwitterionic intermediates exerted by the squaramide through hydrogen bonding. These preliminary studies with compound **3**, in which 44 transition structures were studied and Boltzmann's distributions were applied, also showed that the origin of the diastereoselectivity comes from the *E/Z*-configuration of the second C=C bond of the dienamine. In all cases a conformation *s-trans* is preferred for the dienamine moiety in good agreement with previous studies of Seebach and Uchimaru<sup>[16]</sup> but small differences are observed between *E,E-s-trans* and *E,Z-s-trans* dienamines derived from **4**, thus explaining the low diastereoselectivities observed for this substrate. The attack of the ylide always proceeds by the top face of the dienamine thus

explaining the complete enantioselectivity observed in all cases. Indeed, attack by the bottom face of the catalyst in which no H-bond activation can occur is, in all cases, more than 5.0 kcal/mol higher in energy. Next, we considered the real system used experimentally, i.e. catalyst **2** taking into account both *E,E* and *E,Z* configurations at the dienamine.

The catalytic cycle, illustrated in Scheme 2, begins from the intermediate associated to the catalyst **IN2**, the most stable intermediate in the catalytic cycle, which is formed from the catalyst after initial activation of the two reagents. Calculation of the several possibilities for regenerating **IN2** from the intermediate **IN4**<sup>[17]</sup> showed that the most favourable pathway corresponded to the formation of **IN5** by incorporation of the oxidopyrylium ylide followed by releasing of the product and formation of the dienamine from **IN1** and the aldehyde.



**Scheme 2.** Catalytic cycle for [5+2] cycloaddition catalyzed by **2**.

According to preliminary studies with catalyst **3** the key steps of the reaction are the formation of **IN3** from the initial **IN2**, through **TS1**, and the formation of the final **IN4**, through **TS2**. The rate-limiting step corresponds to the first step involving **TS1**. Hydrolysis to the final product usually takes place smoothly and do not influence the generation of the asymmetric centers formed in previous steps. Eight transition structures, four for each isomer of the dienamine were located for the first step (rate-limiting) of the reaction of (*E*)-2-pentenal **4** catalyzed by **2** (Table 1).<sup>[18]</sup> In all cases the ylide is oriented in the same way as a consequence of the activation by the squaramide moiety through a double hydrogen-bonding. Attack on the top face of the *E,E-s-trans* dienamine (*Re*-face) gives the major product observed experimentally (*5R,6R,7R,8S*-isomer). On the contrary, attack on the top face of *E,Z-s-trans* dienamine (*Si* face) forms the diastereomeric minor compound (*5R,6S,7R,8S*-isomer). Moreover, the pyrrolidine ring of the catalyst can adopt two

different conformations, named North (N) and South (S) that should be considered as different transition structures even though they do not affect the reaction outcome. Also, two different modes of addition have been found, i.e.: the bis-3,5-(trifluoromethyl)benzyl group can be directly above the ylide favoring  $\pi$ - $\pi$  stacking (pocket-like model, PM), or it can point away the ylide (T-like model, TM). Figure 2 illustrates these models for (*E*)-2-pentenal **4**, in particular the two more stable **TS1a** and **TS1d** for the predominant 5*R*,6*R*,7*R*,8*S*-isomer.

**Table 1.** Calculated relative Gibbs energies and percentage of located transition structures for the transformation of **IN2** into **IN3** (R = Me, catalyst **2**)

dienamine	pyrrolidine <sup>[a]</sup>	model <sup>[b]</sup>	TS	$\Delta\Delta G_{rel}^{[c]}$	[%]	product	d.r.
<i>E,E</i> - <i>s-trans</i>	N	PM	<b>TS1a</b>	0.0	40	5 <i>R</i> ,6 <i>R</i> ,7 <i>R</i> ,8 <i>S</i>	68
	N	TM	<b>TS1b</b>	1.6	3		
	S	PM	<b>TS1c</b>	0.9	8		
	S	TM	<b>TS1d</b>	0.5	17		
<i>E,Z</i> - <i>s-trans</i>	N	PM	<b>TS1e</b>	0.5	17	5 <i>R</i> ,6 <i>S</i> ,7 <i>R</i> ,8 <i>S</i>	32
	N	TM	<b>TS1f</b>	1.8	2		
	S	PM	<b>TS1g</b>	1.5	3		
	S	TM	<b>TS1h</b>	0.8	10		

[a] N and S refer to conformations North ( $^3T_2$ ) and South ( $^2T_3$ ) of the pyrrolidine ring, respectively. [b] PM and TM refer to pocket-like and T-like models. [c] given in kcal/mol.

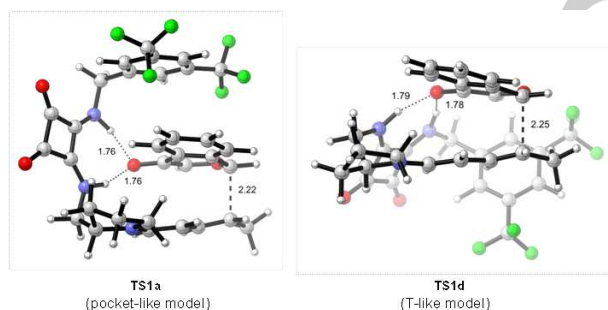


**Figure 2.** Optimized structures for transition states corresponding to the transformation of **IN2** into **IN3** (R = Me, catalyst **2**). Most stable P-model and T-model transition states are shown.

Transition structures in which the pyrrolidine ring adopts a North conformation always prefer the pocket-like model whereas those in which the pyrrolidine ring adopts a South conformation always prefer the T-like model. For both *E,E*-*s-trans* and *E,Z*-*s-trans* dienamines the most stable transition structures are those corresponding to PM model. In this first step of the reaction, two new stereogenic centres are formed at positions 5 and 6 of the final adduct, thus determining the final diastereomeric ratio. The configuration at C-5 is always *R* as a consequence of the attack of the *Si*-face of the ylide by the top face of the dienamine. The configuration at C-6 can be *R* for the attack to the *E,E*-*s-trans* dienamine (by the *Si*-face) or *S* for the attack to the *E,Z*-*s-trans* dienamine (by the *Re*-face). The creation of the two stereogenic

centres at positions 7 (*R*) and 8 (*S*) is fixed by the only possible attack after the first step of the reaction and it takes place through the second step. Boltzmann's distribution of the eight transition structures corresponding to the first step of the reaction gave a theoretical d.r. value of 68:32 in very good agreement with that observed experimentally.<sup>[12]</sup> The small energy differences (less than 1 kcal/mol) between PM and TM models, counting for 40% and 17% of transition structures leading to the major compound, indicates that a distinct preference for one over the other does not take place in a great extent. In fact, during the reaction, pocket-like model is only preferred until the formation of **IN3** in which the T-like model is preferred as well as for **TS2** and **IN4** (for a more detailed analysis see Supporting Information).

An NCI analysis<sup>[19]</sup> for the PM model confirmed the disposition of the catalyst in a rather similar form to an enzymatic pocket in which the reagents are linked covalently (dienamine) and non-covalently (hydrogen-bond) but also in such a form that stabilizing hydrophobic (London dispersion forces) interactions (green surfaces) are present (Figure 3). In this respect the bis-3,5-(trifluoromethyl)phenylmethyl group of catalyst **2** is capable of providing additional  $\pi$ , $\pi$  stacking at both top and bottom faces of the ylide placing it between the dienamine and the aromatic ring. The T-like model also presents favourable London dispersion forces but only between the bottom face of the ylide and the dienamine. Thus, the additional favourable interactions in the pocket-like model contribute to minor stabilization over the T-model (just 0.5 kcal/mol). The N-H-O angles in P-model are 159.3° and 158.4°, and in T-model are 155.0° and 155.4°, in all cases within good values for typical H-bonds of this type.<sup>[7a],[20]</sup>

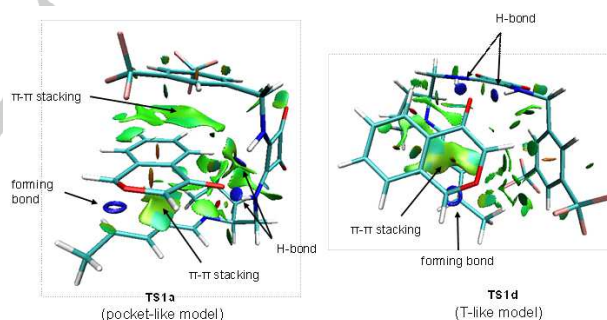


**Figure 3.** NCI models. A forming bond appears as a blue torus. Green surfaces represent favourable delocalized hydrophobic interactions and blue discs represent directional H-bonds.

After the formation of intermediates **IN3**, the reaction proceeds through a second transition state located at 0.8 kcal/mol (for (*E*)-2-pentenal, major diastereomer) below the ground state to form intermediate **IN4**. Figure 4 illustrates the energy profile for the formation of the major isomer in the reaction of (*E*)-2-pentenal **4** and completion of the catalytic cycle. The driving force of the catalytic cycle illustrated in Scheme 2 is determined by the regeneration of **IN2** from **IN4** with concomitant releasing of the final product. This final catalyst-

turnover step involves a favoured energy ( $\Delta G = -6.1$  kcal/mol for the reaction of (*E*)-2-pentenal **4** catalyzed by **2**).

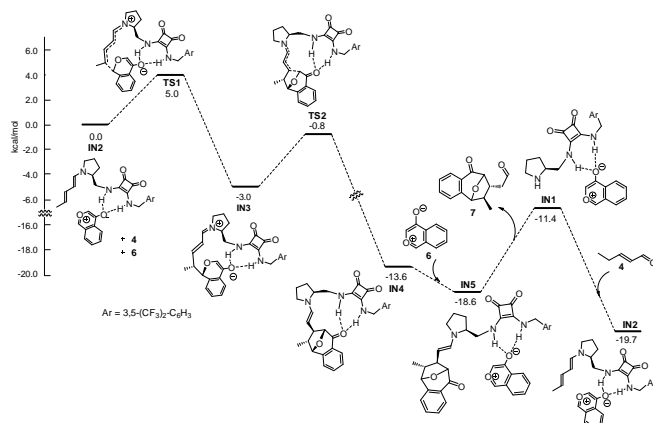


**Figure 4.** Energy surface for the reaction between **4** and **6** catalyzed by **2**. The most stable route corresponding to **TS1a** (from *E,E*-*s-trans*) is shown.

Additional calculations were performed for the reaction between **4** and **6** catalyzed by **1**. In this case, an aryl group is directly linked to the squaramide nitrogen and an orientation favoring a stacking of type dienamine/ylide/aryl group is not possible. The corresponding transition structures for the first step (named as **TS3**) were located and the results are listed in Table 2. As expected, calculations also predict a complete enantioselectivity and moderate diastereoselectivity, since the e.e. is determined by the formation of the H-bonded complex and the d.r. by the initial *E/Z* configuration of the dienamine. In fact, a d.r. value of 77:23 is predicted for catalyst **1**. In this case the most stable transition structure **TS3d** corresponds to a T-like model since no additional favourable  $\pi,\pi$ -stacking can be found. The energy barrier observed for catalyst **1** (4.0 kcal/mol) is lower than that found for catalyst **2** (5.0 kcal/mol), probably because of the higher acidity of squaramide protons. Whereas the reaction between **4** and **6** catalyzed by **2** presented the most stable **TS1a** 6.4 kcal/mol below the ground state (defined as the sum of reagents and catalyst), the same reaction catalyzed by **1** presented the most stable **TS3d** 7.0 kcal/mol below ground state.

**Table 2.** Calculated relative Gibbs energies and percentage of located transition structures for the transformation of **IN2** into **IN3** (R = Me, catalyst **1**)

dienamine	pyrrolidine <sup>[a]</sup>	model <sup>[b]</sup>	TS	$\Delta\Delta G_{rel}^{[c]}$	[%]	product	d.r.
<i>E,E</i> - <i>s-trans</i>	N	PM	<b>TS3a</b>	0.39	22.4	5 <i>R</i> ,6 <i>R</i> ,7 <i>R</i> ,8 <i>S</i>	77
	N	TM	<b>TS3b</b>	1.15	6.3		
	S	PM	<b>TS3c</b>	1.13	6.4		
	S	TM	<b>TS3d</b>	0.00	43.4		
<i>E,Z</i> - <i>s-trans</i>	N	PM	<b>TS3e</b>	1.11	6.7	5 <i>R</i> ,6 <i>S</i> ,7 <i>R</i> ,8 <i>S</i>	23
	N	TM	<b>TS3f</b>	1.80	2.0		
	S	PM	<b>TS3g</b>	1.52	3.3		
	S	TM	<b>TS3h</b>	0.79	11.5		

[a] N and S refer to conformations North ( $^3T_2$ ) and South ( $^2T_3$ ) of the pyrrolidine

ring, respectively. [b] PM and TM refer to pocket-like and T-like models, respectively. [c] given in kcal/mol.

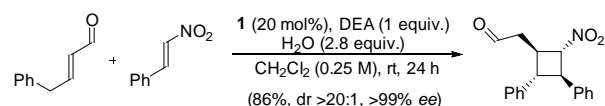
To validate the model we also calculated the eight transition states corresponding to the rate-limiting step of the reaction between **5** and **6** catalyzed by **2**, in which complete enantio- and diastereoselectivity was achieved. Calculations (Table 3) correctly predict the exclusive obtention of the 5*R*,6*S*,7*R*,8*S* isomer, as observed experimentally. For this reaction, the most stable **TS4d** (corresponding to the formation of **IN3** from **IN2**, R = Ph) was found 11.0 kcal/mol below the ground state. Noteworthy, for this reaction the T-like model (and accordingly South conformation in the pyrrolidine ring) is preferred in all TS pairs counting for a 67.5% of all the transition structures. This is due to a shorter distance of the forming bond in **TS3d** (2.05 Å) with respect to the reaction with aldehyde **4** (2.22 Å in **TS1a**) that causes a weakening of the additional  $\pi,\pi$ -interactions of the pocket-like model. The N-H-O angles in P-model are 158.0° and 160.0°, and in T-model are 153.4° and 154.5° in agreement with favourable H-bonding interactions.<sup>[7a,20]</sup> The lower stability of transition structures derived from *E,Z*-*s-trans* dienamine is due to unfavourable steric interactions between the phenyl group and the coplanar ethylenic protons of the dienamine. In fact, the phenyl ring is not completely planar (dihedral angle of -18.5°) with the dienamine as a consequence of such interactions.

**Table 3.** Calculated relative Gibbs energies and percentage of located transition structures for the transformation of **IN2** into **IN3** (R = Ph, catalyst **2**)

dienamine	pyrrolidine <sup>[a]</sup>	model <sup>[b]</sup>	TS	$\Delta\Delta G_{rel}^{[c]}$	[%]	product	d.r.
<i>E,E</i> - <i>s-trans</i>	N	PM	<b>TS4a</b>	1.0	12.6	5 <i>R</i> ,6 <i>R</i> ,7 <i>R</i> ,8 <i>S</i>	99.9
	N	TM	<b>TS4b</b>	0.8	16.2		
	S	PM	<b>TS4c</b>	1.7	3.6		
	S	TM	<b>TS4d</b>	0.0	67.5		
<i>E,Z</i> - <i>s-trans</i>	N	PM	<b>TS4e</b>	4.3	0.0	5 <i>R</i> ,6 <i>S</i> ,7 <i>R</i> ,8 <i>S</i>	0.1
	N	TM	<b>TS4f</b>	5.8	0.0		
	S	PM	<b>TS4g</b>	5.2	0.0		
	S	TM	<b>TS4h</b>	4.1	0.1		

[a] N and S refer to conformations North ( $^3T_2$ ) and South ( $^2T_3$ ) of the pyrrolidine ring, respectively. [b] PM and TM refer to pocket-like and T-like models, respectively. [c] given in kcal/mol.

The above-discussed modes of activation for catalysts **1** and **2** can also be extended to other systems different than the pyrilium ylide **6**. Thus, we applied our models to the formal [2+2] cycloaddition between  $\alpha,\beta$ -unsaturated aldehydes and nitroalkenes catalyzed by **1** (Scheme 4).<sup>[8]</sup>



**Scheme 4.** Formal [2+2] cycloaddition between  $\alpha,\beta$ -unsaturated aldehydes and nitroalkenes catalyzed by **1**.<sup>[8]</sup>

It was possible to replace the pyrilium ylide by the nitroalkene and locate the corresponding transition structures (Figure 4). In the case of the reaction catalyzed by **1**, a typical<sup>[7a,21]</sup> H-bond interaction between squaramide and nitro group with both oxygen atoms acting as proton acceptors was found (**TS-nitro1**). The preferred model for catalyst **2** was again directed by the flexibility of the arylmethyl group which induces a different H-bonding pattern involving of only one oxygen atom of the nitro group (**TS-nitro2**). This is due to favourable  $\pi, \pi$ -interactions between the aryl group and the N=O bond (oxygen atom not involved in interaction with the squaramide) which can, indeed, be considered to be a double bond. Consequently, the oxygen atom should develop a negative charge,<sup>[22]</sup> thus promoting the type of interaction with the squaramide showed in **TS-nitro2**, more typical for carbonyl oxygen atoms.<sup>[7a]</sup> The interaction between N=O and aryl group has been evidenced by a NCI analysis (see Supporting Information). On the other hand, in **TS-nitro1** a typically delocalized structure of the nitro group is more in agreement with the observed interaction. Both **TS-nitro1** and **TS-nitro2** are the most stable and they account for 100% of abundance for the reaction catalyzed by **1** and **2**, respectively, thus predicting complete diastereo- and enantioselectivity as described experimentally for **1**.<sup>[8]</sup>

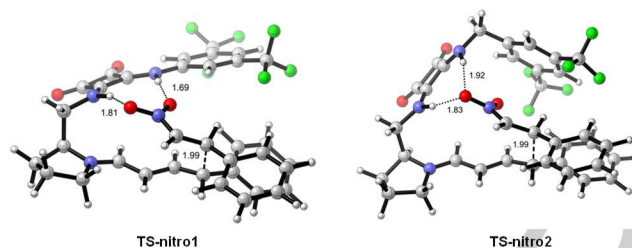


**Figure 4.** Optimized structures for the most stable transition states corresponding to the formal [2+2] cycloaddition between  $\alpha, \beta$ -unsaturated aldehydes and nitroalkenes catalyzed by **1** (left) and **2** (right).

In conclusion, calculations correctly predict the complete enantioselectivity observed experimentally for the [5+2] cycloaddition catalyzed by **2**. The different d.r. observed for aldehydes **4** and **5** are also correctly predicted. The mechanistic picture showed the possibility of two different modes of action, the so-called pocket-like model (P-model) and T-like model (T-model). In catalyst **3** where no aromatic residues are present, T-model is clearly preferred, P-model being ca. 3-4 kcal higher in energy in the corresponding TSs. A similar situation is observed for catalyst **1** because the aromatic ring is directly bonded to the squaramide nitrogen. The additional methylene group in catalyst **2** provides enough flexibility for adopting P-model in which  $\pi, \pi$ -interactions can be established. These additional hydrophobic forces make P-model competitive in the reaction between **4** and **6** and more stable than T-model although by only 0.5 kcal/mol. Indeed, since  $\pi, \pi$ -interactions (London dispersion forces) are the weakest of all the intermolecular forces and they decrease rapidly with the distance, the T-model is preferred over the P-model in the reaction between **5** and **6** because the aromatic rings move away. The influence of the acidity of the NH-groups may also affect the reactivity and, while similar acidity should be expected for catalysts **2** and **3** and thus similar barriers for the

rate-limiting step have been observed, the increased acidity expected for catalyst **1** turns into a lower barrier by 1.0 kcal/mol. Finally, these modes of action found for catalysts **1** and **2** can also be extended to other related systems.

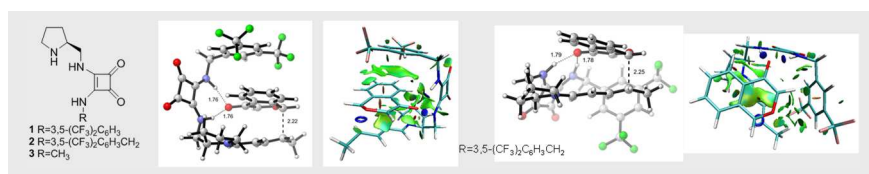
## Acknowledgements

This work was supported by Spanish MINECO Contracts CTQ2013-44367-C2-1-P (to P.M.) and CTQ2014-52107 (to J.L.V.). We also acknowledge the Government of Aragón (Spain) (Group E-10), the Basque Government (Spain) (IT328-10) and Aarhus University (Denmark) for financial support. We acknowledge the Institute of Biocomputation and Physics of Complex Systems (BIFI) at the University of Zaragoza (Spain) for computer time at clusters Terminus and Memento. D.R.-L. thanks the Spanish Ministry of Education (MEC) for a predoctoral grant (FPU program).

**Keywords:** Asymmetric catalysis • DFT calculations • Organocatalysis • Dienamines • Ylides

- [1] B. M. Trost, *Proc. Nat. Acad. Sci. USA* **2004**, *101*, 5348-5355.
- [2] A. Milo, A. J. Neel, F. D. Toste, M. S. Sigman, *Science* **2015**, *347*, 737-743.
- [3] *Sci. Synth.: Asymmetric Organocatalysis*; two-volume set (Eds.: B. List, K. Maruoka), Thieme, 2012.
- [4] L.-Q. Lu, X.-L. An, J.-R. Chen, W.-J. Xiao, *Synlett* **2012**, *23*, 490-508.
- [5] (a) T. Inokuma, Y. Takemoto, *Sci. Synth., Asymmetric Organocatalysis* **2012**, *2*, 437-497. (b) O. V. Serdyuk, C. M. Heckel, S. B. Tsogoeva, *Org. Biomol. Chem.* **2013**, *11*, 7051-7071. (c) X. Fang, C.-J. Wang, *Chem. Commun.* **2015**, *51*, 1185-1197.
- [6] M. Tsakos, C. G. Kokotos, *Tetrahedron* **2013**, *69*, 10199-10222.
- [7] (a) P. Chauhan, S. Mahajan, U. Kaya, D. Hack, D. Enders, *Adv. Synth. Catal.* **2015**, *357*, 253-281. (b) J. Aleman, A. Parra, H. Jiang, K. A. Jørgensen, *Chem. Eur. J.* **2011**, *17*, 6890-6899.
- [8] L. Albrecht, G. Dickmeiss, F. Cruz Acosta, C. Rodriguez-Esrich, R. L. Davis, K. A. Jørgensen, *J. Am. Chem. Soc.* **2012**, *134*, 2543-2546.
- [9] (a) L. Albrecht, G. Dickmeiss, C. F. Weise, C. Rodriguez-Esrich, K. A. Jørgensen, *Angew. Chem., Int. Ed.* **2012**, *51*, 13109-13113. (b) C. F. Weise, V. H. Lauridsen, R. S. Rambo, E. H. Iversen, M.-L. Olsen, K. A. Jørgensen, *J. Org. Chem.* **2014**, *79*, 3537-3546.
- [10] B. S. Donslund, K. S. Halsvov, L. A. Leth, B. M. Paz, K. A. Jørgensen, *Chem. Commun.* **2014**, *50*, 13676-13679.
- [11] H. Jiang, C. Rodriguez-Esrich, T. K. Johansen, R. L. Davis, K. A. Jørgensen, *Angew. Chem., Int. Ed.* **2012**, *51*, 10271-10274.
- [12] A. Orue, U. Uria, E. Reyes, L. Carrillo, J. L. Vicario, *Angew. Chem. Int. Ed.* **2015**, *54*, 3043-3046.
- [13] (a) L. Albrecht, C. V. Gomez, C. B. Jacobsen, K. A. Jørgensen, *Org. Lett.* **2013**, *15*, 3010-3013. (b) L. Albrecht, F. C. Acosta, A. Fraile, A. Albrecht, J. Christensen, K. A. Jørgensen, *Angew. Chem., Int. Ed.* **2012**, *51*, 9088-9092.
- [14] T. Lu, S. E. Wheeler, *Chem. Eur. J.* **2013**, *19*, 15141-15147.
- [15] The use of B3LYP functional with dispersion correction (D3) in conjunction with TZVP basis has provided excellent results in organocatalytic reactions: A. Armstrong, R. A. Boto, P. Dingwall, J. Contreras-Garcia, M. J. Harvey, N. J. Masona, H. S. Rzepa, *Chem. Sci.* **2014**, *4*, 2057-2071. Unless otherwise noted, the relative energies reported in the text correspond to relative free energies computed at B3LYP-D3BJ/Def2TZVP// B3LYP-D3BJ/Def2SVP level in THF solvent (PCM).

- [16] U. Groselj, D. Seebach, D. M. Badine, W. B. Schweizer, A. K. Beck, I. Krossing, P. Klose, Y. Hayashi, T. Uchimaru, *Helv. Chim. Acta* **2009**, *92*, 1225-1259.
- [17] Transformation of **IN4** into **IN2** requires: i) releasing of the product through decoordination and hydrolysis, ii) coordination of the ylide and iii) formation of the dienamine. All these events can take place in different order affording diverse intermediates. For the full study considering all the pathways see Supporting Information.
- [18] A total of 24 transition structures were evaluated but only 8 of them correspond to an abundance of 100% (Boltzmann's distribution)
- [19] (a) E. R. Johnson, S. Keinan, P. Mori-Sanchez, J. Contreras-Garcia, A. J. Cohen, W. Yang, *J. Am. Chem. Soc.* **2010**, *132*, 6498-6506. (b) J. R. Lane, J. Contreras-Garcia, J.-P. Piquemal, B. J. Miller, H. G. Kjaergaard, *J. Chem. Theory Comput.* **2013**, *9*, 3263-3266.
- [20] (a) A. Berkessel, K. Etzenbach-Effers In *Hydrogen bonding in Organic Synthesis*, P. M. Pihko (Ed.), Wiley-VCH. Weinheim. 2009, pp. 15-42 (b) R. I. Storer, C. Aciro, L. H. Jones, *Chem. Soc. Rev.* **2011**, *40*, 2330-2346. (c) P. Merino, I. Delso, T. Tejero, D. Roca-López, A. Isasi, R. Matute, *Curr. Org. Chem.* **2011**, *15*, 2184-2209.
- [21] (a) H. Klare, J. M. Neudorfl, B. Goldfuss, *Beilstein J. Org. Chem.* **2014**, *10*, 224-236. (b) W. R. Zheng, J. L. Xu, T. Huang, Q. Yang, Z. C. Chen, *Res. Chem. Intermed.* **2011**, *37*, 31-45.
- [22] In fact, whereas Mulliken charges for oxygen atoms of the nitro group are similar in **TSnitro1** (-0.405 and -0.409), in **TSnitro2** the atom involved in  $\pi,\pi$ -interactions has less negative charge (-0.356) than that involved in H-bond (-0.443).



*D. Roca-López, U. Uria, E. Reyes, L. Carrillo, K. A. Jørgensen, J. L. Vicario\* and Pedro Merino\**

**Page No. – Page No.**

**Mode of Action of Bifunctional Squaramide Organocatalysts**

Two primary modes of action depending on favourable  $\pi,\pi$ -interactions are possible for bifunctional pyrrolidine squaramide-derived organocatalysts. The model can be applied to several reactions including [5+2] and [2+2] cycloadditions.

WILEY-VCH